NASCAP/LEO CALCULATIONS OF CURRENT COLLECTION

M. J. Mandell, I. Katz, V. A. Davis, R. A. Kuharski

S-CUBED, A Division of Maxwell Laboratories, Inc.
P. O. Box 1620, La Jolla, California 92038

Abstract. NASCAP/LEO is a 3-dimensional computer code for calculating the interaction of a high-voltage spacecraft with the cold dense plasma found in Low Earth Orbit. Although based on a cubic grid structure, NASCAP/LEO accepts object definition input from standard CAD programs so that a model may be correctly proportioned and important features resolved. The potential around the model is calculated by solving the finite element formulation of Poisson's equation with an analytic space charge function.

Five previously published NASCAP/LEO calculations for three ground test experiments and two space flight experiments are presented. The three ground test experiments are a large simulated panel, a simulated pinhole, and a 2-slit experiment with overlapping sheaths. The two space flight experiments are a solar panel biased up to 1000 volts, and a rocket-mounted sphere biased up to 46 kilovolts. In all cases, we find good agreement between calculation and measurement.

Introduction

This report is an expanded version of a poster presentation made at the "Workshop on Current Collection from Space Plasmas," Huntsville, Alabama, April 24-25, 1989. The objective of this document is to summarize the capabilities and the physical and numerical basis of the NASCAP/LEO computer code. NASCAP/LEO is capable of calculating the potential and sheath structure around a geometrically and electrically complex spacecraft immersed in a plasma, and the plasma currents collected by the surfaces of such an object.

We present here five previously published case studies of NASCAP/LEO simulations of experiments studying interactions of charged surfaces with a plasma representative of Low Earth Orbit. Three of the experiments were performed under ground test conditions, and two were for actual space flights. As the first four cases were done with an older version of NASCAP/LEO that required that objects be made of cubes, these objects were redefined and a few calculations performed to illustrate NASCAP/LEO's present capabilities. All the new calculations agreed with the previously published results.

NASCAP/LEO features the ability to accept a general geometrical description of the spacecraft or test object. The spacecraft is defined as a finite element surface model using a standard CAD finite element generator such as Patran[a] or EMRC[b] Display-II. An interface code reads the "neutral file" output by the finite element generator and places the object in a cubic grid. Variable surface resolution is naturally achieved in the finite element generator; locally enhanced spatial resolution is available via directive to the interface code. The object may be defined with correct angles and proportions independent of the cubic grid resolution.

NASCAP/LEO is designed to calculate space potentials in the regime where the applied voltages are large compared to the plasma temperature, and the Debye length is comparable to,or less than, the code resolution. A local space charge formulation takes account of plasma screening and acceleration and convergence of charged particles such that the Langmuir-Blodgett result will be reproduced for a spherical sheath. Currents flowing from the sheath to the object are calculated taking into account ram-wake and magnetic field effects.

NASCAP/LEO also has specialized modules to calculate spacecraft floating potentials, surface charging, mean potential of a solar array surface, parasitic power loss of a solar-voltaic power system, and hydrodynamic ion flow about a spacecraft.

Physical and Numerical Basis of NASCAP/LEO

NASCAP/LEO is a 3-dimensional computer code that can calculate self-consistently electrostatic potentials surrounding a charged object, plasma currents incident on object surfaces, and object surface potentials for plasma conditions appropriate to low earth orbit.

The electrostatic potential, ϕ, about the object is determined by solving Poisson's equation

$$-\nabla^2\phi = \rho/\varepsilon_0 \qquad (1)$$

subject to fixed potential or fixed electric field boundary conditions at object surfaces. (These boundary conditions may be set by the user, or by other modules of NASCAP/LEO.) The space charge, ρ, appearing in Poisson's equation is approximated as a nonlinear analytic function of the plasma properties and the local potential and electric field. The function used is

(a) Patran is a trademark of PDA Engineering, Costa Mesa, CA.
(b) Engineering Mechanics Research Corporation, Troy, MI.

$$\rho(\phi,E)/\varepsilon 0 = -(\phi/\lambda^2) \times [1+C(\phi,E)\phi] \times [1+(4\pi)^{1/2}|\phi/\theta|^{3/2}]^{-1} \quad (2)$$

where the first factor represents linear screening with Debye length λ, the second represents increase in density due to trajectory convergence (where the convergence factor $C(\phi,E)$ is a function of local field and potential calculated to give the correct answer for a Langmuir-Blodgett spherical sheath), and the third represents decrease in density due to particle acceleration, with θ being the plasma temperature [eV]. An algorithm is included to account for ram-wake effects in the neutral particle approximation.

NASCAP/LEO solves the variational form of Poisson's equation

$$\delta \int d^3\mathbf{r} \left\{ (\varepsilon_0/2)|\nabla\phi|^2 + \rho\phi \right\} = 0 \quad (3)$$

using the finite element method and a conjugate gradient technique for sparse linear equations. After each solution of the linear equations, the nonlinear space charge is linearized about the current solution, and the new equations solved. This process is continued until the solution is deemed sufficiently near a fixed point.

The finite element method works well for this problem because most of space is filled with trilinear "empty" elements. "Stiffness matrices" for those elements containing surfaces are constructed numerically. The potential solver allows "nested outer grids" in order to include a large volume of space, and "subdivided inner grids" to achieve locally enhanced resolution where needed.

NASCAP/LEO calculates currents to a charged object using the "sharp sheath edge" approximation. The "sharp sheath edge" is a specified equipotential surface (usually $\pm\theta ln2$). Macroparticles representing ion and/or electron currents are generated for each element of sheath area, taking ram-wake effects into account. These macroparticles are tracked in the electric fields resulting from the Poisson solution, and user-specified magnetic fields, to determine where (or whether) they strike the object.

Potentials of insulating surfaces are calculated to achieve current balance among the incident (sheath and thermal) ions and electrons, and the secondary electrons. For insulators near high positive voltage surfaces, we use an electric field boundary condition which represents

equilibrium between incident electrons and transport of secondary electrons along the surface. This boundary condition is given by

$$\mathbf{E}\cdot\mathbf{n} = [4 \langle\varepsilon\rangle \gamma \nabla\cdot\mathbf{E}_{\|}]^{1/2} \qquad (4)$$

where $\langle\varepsilon\rangle$ is the mean energy of secondary electrons and γ is the secondary yield for primary electrons with energy equal to the surface potential.

A solar array surface is an important example of a complex surface that is a mosaic of dielectric (coverslips) and conductor (interconnects). Because of the obvious importance of solar arrays on spacecraft, we have developed an algorithm, based on equation (4), to calculate self-consistently the mean potential and mean electric field for a periodic surface. This algorithm, which takes advantage of the periodic structure of solar arrays, is discussed further in section 6 below.

Example 1: Simulated Solar Panel (1980)(Katz et al., 1981)

The first NASCAP/LEO paper ever published reported simulation of measurements by McCoy and Konradi (1979) of current collection by a 10-meter long "panel" exposed to an argon plasma in the large vacuum chamber at Johnson Space Center. The "panel" was actually a conducting strip mounted on a plastic frame. The strip could be held at fixed constant potential or could maintain a linear potential gradient along its length.

Figure 1 shows the NASCAP/LEO model of the panel. This model was constructed using EMRC Display-II. Note the variable resolution across the width of the panel, giving good resolution of the metal-plastic interface. Variable resolution is also used lengthwise near the ends. Figure 2 shows the same panel with linear bias (in ten steps) from zero to -4,800 volts.

Figure 3 shows the plasma potentials around the panel for the bias shown in figure 2. The plasma conditions used in the calculation were plasma density $n = 1.3 \times 10^6$ cm^{-3}, and plasma temperature $\theta = 2.3$ eV. The sheath shape is in agreement with what was visually observed. The primary grid unit is 0.333 meters. Note the locally enhanced resolution used near the panel surface.

The calculation also gives the current density on the panel surface, which is strongly enhanced at the high voltage end. The total current collected was 26 milliamperes, which compares well with a measurement of "slightly under" 20 milliamperes when the panel was biased from zero to -4,000 volts.

Example 2: Simulated Pinhole (1983)(Mandell and Katz, 1983)

It is well accepted that a small, positively biased conducting surface can collect current out of proportion to its size if surrounded by dielectric material. This is because secondary electron emission facilitates the spread of high positive voltage from the conductor onto the surrounding insulator. NASCAP/LEO models this phenomenon by requiring current balance between the incident electron current and the divergence of the current carried by the secondary electron layer. As the latter is proportional to the incident electron current and a strong function of the normal electric field at the surface, the potential at the dielectric surface is determined by imposing the boundary condition of a small (but nonzero) outward pointing electric field, whose value is given by equation (4).

Experiments performed by Gabriel et al.(1983) made an excellent test of the treatment of this phenomenon by NASCAP/LEO. The experiment fixture was kapton-covered except for a circular region of diameter either 1.27 cm or 0.64 cm. The experimenters measured the potentials in the plasma along the "pinhole" axis. For the smaller pinhole, the collected current was measured.

Figure 4 shows the surface potentials on the NASCAP/LEO model of the fixture with the larger pinhole. The model was constructed using EMRC Display-II, and has good resolution in the region surrounding the pinhole. (A similar model was constructed for the smaller pinhole.) The pinhole was biased to +458 volts in a plasma with $n = 5.8 \times 10^4$ cm^{-3}, $\theta = 4$ eV. The spread of high potential onto the insulator is clearly seen.

Figure 5 shows the potentials in space above the pinhole for the same case. The NASCAP/LEO results are compared with experiment in figure 6, which is taken from the original paper (Mandell and Katz, 1983).

For the smaller pinhole, the experimenters measured a collected current of 4 μA when the pinhole was biased to 458 volts in a plasma with $n = 2.5 \times 10^4$ cm^{-3}, $\theta = 5.3$ eV. This value approaches the orbit-limited value of 4.2 μA, and is far in excess of the planar current estimate of 0.05 μA. The collection of orbit-limited current is consistent with a zero electric field boundary condition on the dielectric. The NASCAP/LEO calculated current is 2.4 μA.

Example 3: Overlapping Sheaths (1987)(Davis et al., 1988)

A related experiment was performed by Carruth.(1987). Rather than the pinhole geometry, Carruth measured collected current and plasma potential for the more complex geometry of two parallel slits. Carruth used relatively low voltages

so as to avoid "snapover". (At higher voltages, a sharp increase in current, indicating snapover, was observed.)

Figure 7 shows the NASCAP/LEO model of Carruth's experiment with biases of 128 and 328 volts on the slits. Once again, this model was constructed using EMRC Display-II. Though it is not apparent from the figure, the model was constructed such that the current collected by the central 4.2 cm of each slit could be calculated, the same quantity measured in the experiment. Figure 8 shows a sheath contour plot for plasma conditions $n = 2 \times 10^6$ cm^{-3}, $\theta = 2$ eV. (The primary grid spacing used for this calculation was 1.429 cm.) The figure shows that the sheaths of the two slits do indeed overlap. The calculated potentials agree well with the experimental measurements.

Figure 9 [taken from the original paper (Davis et al., 1988)] shows the current collected by each of the two slits when one is held at 100 volts and the potential of the other is varied. Agreement between experiment and calculation is excellent.

Example 4: PIX-II Flight Experiment (1983) (Mandell et al., 1986)

PIX-II (Grier, 1985) was an orbital experiment designed to measure the interaction of a high-voltage (up to ±1,000 volts) solar array with the plasma environment. The instrumentation consisted of a 2,000 cm^2 passive solar array whose interconnects could be biased relative to the rocket ground, a Langmuir probe, and a hot-wire neutralizer. The results showed that current collection was enhanced by the "snapover" effect at positive biases over a few hundred volts, and that arcing occurred at negative biases as low as 250 volts.

In modeling the PIX-II experiment, it rapidly became apparent that it was not possible to resolve in detail a surface consisting of 2 cm x 2 cm solar cells with 0.1 cm interconnects. Strategies such as lumping the many interconnects together into a few surface zones gave a grossly inadequate representation of the surface. Therefore, taking into account that a solar array surface is a periodic structure, an analytic representation of this surface was developed. The physical content of this solar array surface model is that a dielectric in a cold plasma can achieve current balance either (1) at negative potential such that ion and electron currents balance, or (2) at small, positive electric field (given by equation (4)), provided that the resulting potential is high enough to produce secondary electron yield greater than unity. When the coverslips are in the latter condition due to the presence of high-voltage interconnects, the coverslip potential profile must be such that the positive (electron-attracting) mean electric field

must be approximately canceled by the spatially periodic components. These ideas lead to a formulation that calculates the mean potential of the surface self-consistently with the mean electric field returned from NASCAP/LEO's Poisson solver. Its parameters include the cell size, interconnect size, and coverslip material properties. (Mathematical details may be found in Mandell et al., 1986.) Thus NASCAP/LEO is capable of predicting the "snapover" (or partial snapover) of the coverslips in response to high positive interconnect potentials, without explicitly resolving the coverslips and interconnects.

Figure 10 shows the NASCAP/LEO model of PIX-II, constructed using EMRC Display-II. This model is not based directly on the PIX-II rocket, but rather on the original NASCAP/LEO model of PIX-II. It differs from the original model in that the rocket is round rather than square, and that the change in resolution approaching the experiment takes place smoothly rather than suddenly.

Figure 11 shows the surface potentials on the experiment with the interconnects biased to 1,000 volts. Most of the solar cells were calculated to have mean potential in the range of 700-850 volts. For this case, the rocket structure ground was taken to be at -4 volts, and the interconnects comprised 5 percent of the cell area. Thus, we infer a mean coverslip potential of about 150-300 volts below the interconnect potential.

Figure 12 shows the current collected by the solar array as a function of bias voltage. (This figure is taken from the original publication.) The calculated values are in general agreement with the measurements. The calculation exhibits a sharper snapover at lower potential than was measured because calculations were done in a manner which tends to favor the bistable snapped-over state, while the experiment was done by continuously increasing the bias which tends to suppress the snapover.

Example 5: SPEAR I Rocket Experiment (1987) (Katz et al., 1989)

The SPEAR (Space Power Experiments Aboard Rockets) program has as its objective the development of technology for efficient design of very high voltage and current systems to operate in the space environment. The SPEAR I experiment consisted of two boom-mounted probes that could be biased up to 46 kilovolts positive relative to the rocket body. It was intended that the rocket body would maintain good contact with the ambient plasma via a hollow cathode plasma contactor. However, the contactor was defeated by a mechanical malfunction, so that the rocket body became negatively charged, and the experiment was far less

symmetric than planned. NASCAP/LEO proved the utility of a general 3-dimensional modeling capability to understand the results of this nonsymmetric flight experiment.

Figure 13 shows the NASCAP/LEO model of SPEAR I with a 46 kilovolt bias on one sphere and the rocket body at its floating potential of -8 kilovolts. The model was constructed using Patran. Figure 14 is a sheath contour plot showing the asymmetric sheath formed by SPEAR I under the above bias conditions. The plasma conditions for this calculation were $n = 1 \times 10^5$ cm^{-3} and $\theta = 0.1$ eV. The primary grid unit is 0.3 meters, and the resolution in the region of the spheres is 7.5 centimeters.

Because the sheath is not symmetric about the sphere, theoretical results about the role of magnetic field in limiting currents to spheres cannot be directly applied. Figure 15 shows the trajectory of an electron in a potential similar to that shown. The electron **ExB** drifts around the surface of the sheath until (unlike the symmetric case) it enters a high electric field region and is collected. Figure 16 shows the NASCAP/LEO calculated electron current to the sphere and the secondary-electron-enhanced ion current to the rocket as a function of rocket potential. As the potential goes negative, the electron current first increases due to loss of symmetry, then decreases due to the ion-collecting sheath engulfing the electron-collecting sheath. Figure 17 shows the excellent agreement between the measured current and the NASCAP/LEO calculation.

While NASCAP/LEO takes account of the effect of magnetic fields on particle trajectories and thus collected currents, it ignores the effect of magnetic fields on the space charge and potential structure. For comparison, the POLAR code was run for the one case above to achieve self-consistent space-charge, potential, and current solutions in the presence of the magnetic field. The differences found were fairly insignificant.

Summary

NASCAP/LEO is a 3-dimensional computer code capable of calculating sheath structure, surface potentials, and current collection for a high-voltage object in a plasma. The ability to accept object definition input from standard CAD programs allows spacecraft or test object models to be correctly proportioned with important features adequately resolved. The cubic grid structure and the analytic space charge representation, together with phenomenological models for other relevant physical phenomena (such as snapover), permit realistic calculations to be performed in modest amounts of computer time.

We have highlighted in this report five previously published NASCAP/LEO calculations. These examples show that it is practical to perform calculations for nonsymmetric, 3-dimensional, realistic problems. They also verify that NASCAP/LEO results stand the test of direct comparison with measurement for both ground test and space flight conditions.

Acknowledgements. This work has been supported by NASA/Lewis Research Center under contract NAS3-23881.

References

Katz, I., M. J. Mandell, G. W. Schnuelle, D. E. Parks, and P. G. Steen, Plasma collection by high-voltage spacecraft in low earth orbit, J. Spacecraft, 18, 79, 1981.

McCoy, J. E. and A. Konradi, Sheath effects observed on a 10 meter high voltage panel in simulated low earth orbit, Spacecraft Charging Technology-1978, NASA CP-2071, 341, 1979.

Mandell, M. J. and I. Katz, Potentials in a plasma over a biased pinhole, IEEE Trans. Nucl. Sci., NS-30, 4307, 1983.

Gabriel, S. B., C. E. Garner and S. Kitamura, Experimental measurements of the plasma sheath around pinhole defects in a simulated high-voltage solar array, AIAA Paper No. 83-0311, AIAA 21st Aerospace Sciences Meeting, Reno, NV, January 10-13, 1983.

Davis, V. A., M. J. Mandell and I. Katz, Electron collection by multiple objects within a single sheath, J. Spacecraft, 25, 94, 1988.

Carruth, M. R., Jr., Plasma electron collection through biased slits in a dielectric, J. Spacecraft, 24, 79, 1987.

Mandell, M. J., I. Katz, G. A. Jongeward, and J. C. Roche, Computer simulation of plasma electron collection by PIX-II, J. Spacecraft, 23, 512, 1986.

Grier, N. T., Plasma Interaction Experiment II: laboratory and flight results, in proceedings of Spacecraft Environment Interactions Technology Conference, Colorado Springs, CO, October 4-6, 1983, NASA CP-2359, 333, 1985).

Katz, I., G. A. Jongeward, V. A. Davis, M. J. Mandell, R. A. Kuharski, J. R. Lilley, Jr., W. J. Raitt, D. L. Cooke, R. B. Torbert, G. Larson, and D. Rau, Structure of the bipolar plasma sheath generated by SPEAR I, J. Geophy. Res., 94, 1450, 1989.

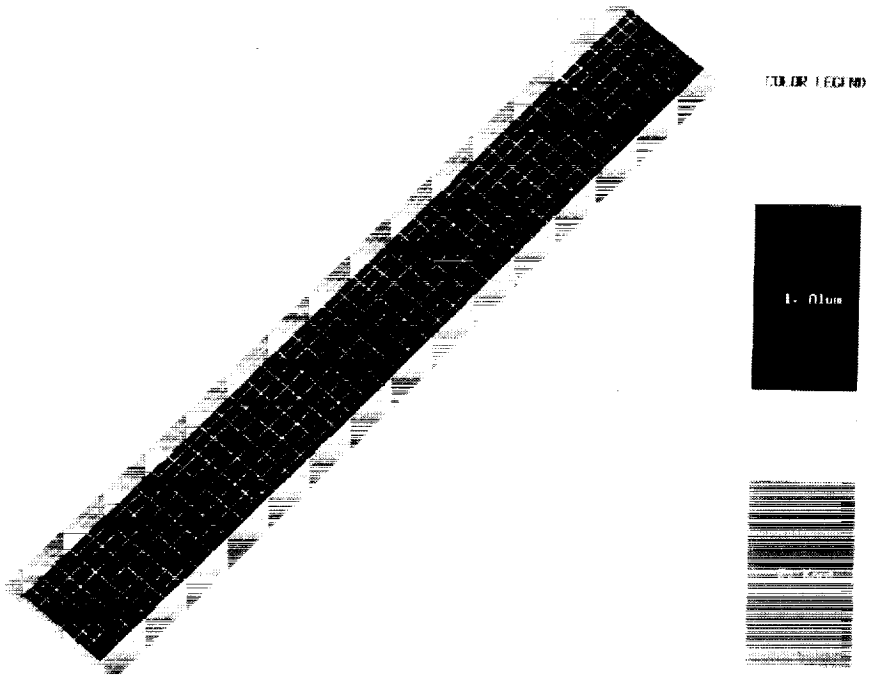

Figure 1 NASCAP/LEO model of a 10-meter simulated solar panel, consisting of a conductive strip mounted on a plastic frame.

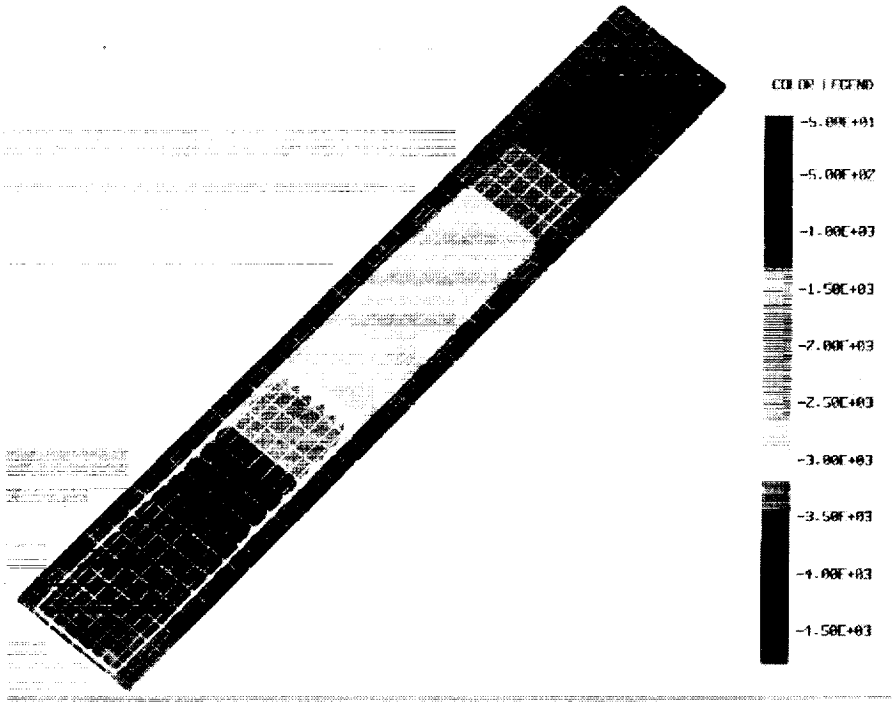

Figure 2 The simulated solar panel (mounted on a plastic frame) is shown with a uniform (in ten steps) potential gradient from zero to -4,800 volts.

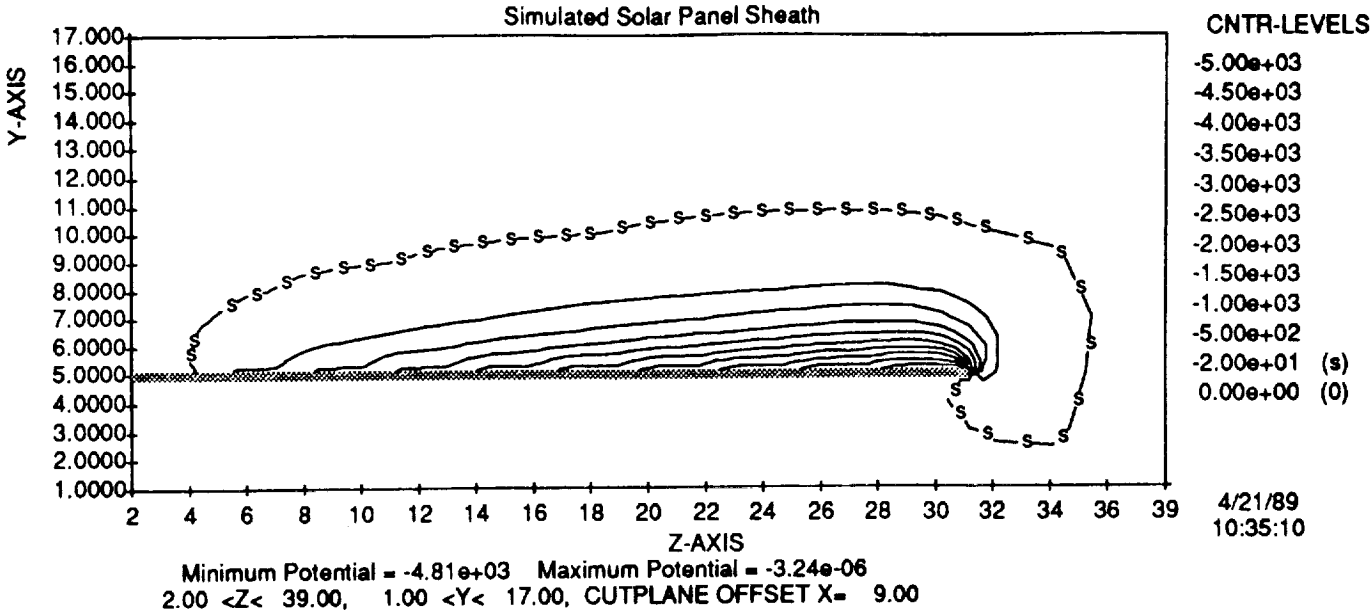

Figure 3 NASCAP/LEO results for the plasma sheath around the simulated solar panel. (Note that the dark blue region consists of potentials from -4,800 volts to -100 volts.)

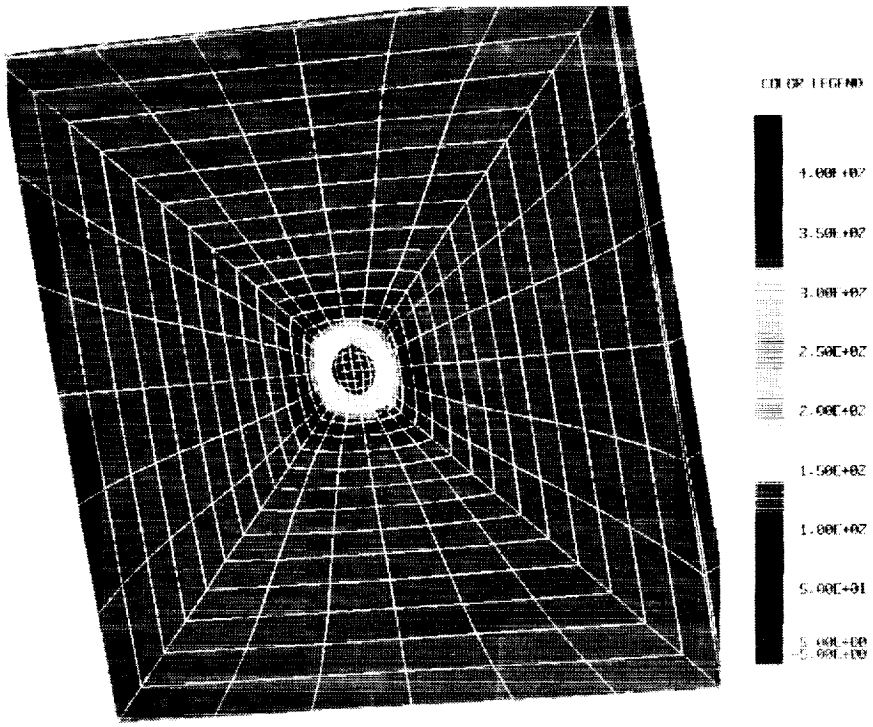

Figure 4 NASCAP/LEO model of the experimental fixture with a 1.27 cm diameter pinhole biased to 458 volts, showing surface potentials. Note the spread of high voltage onto the surrounding insulation.

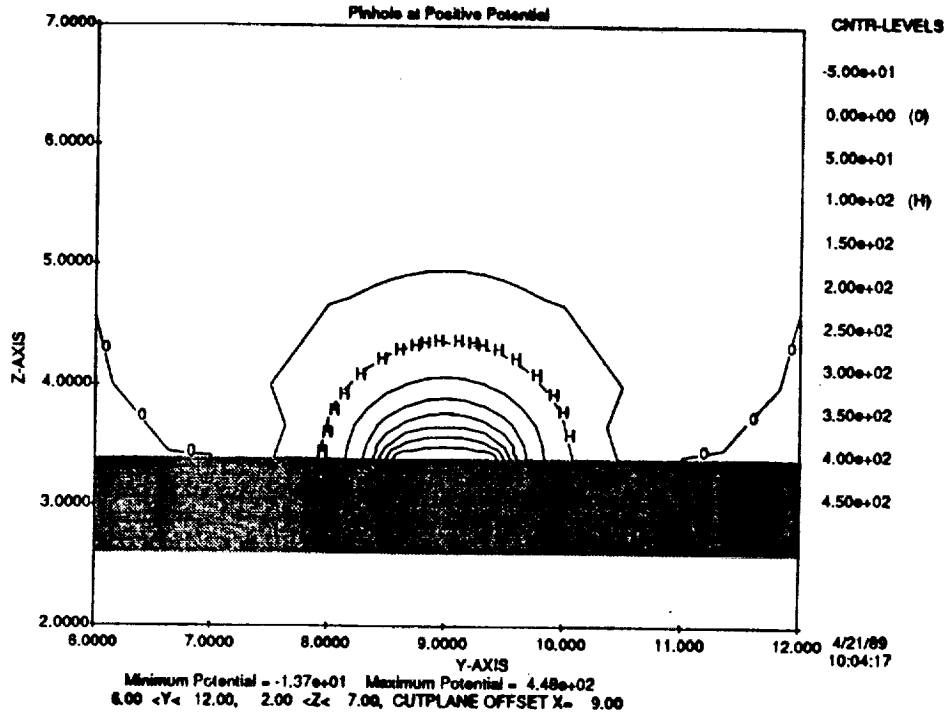

Figure 5 NASCAP/LEO results for potentials in the plasma above the simulated pinhole.

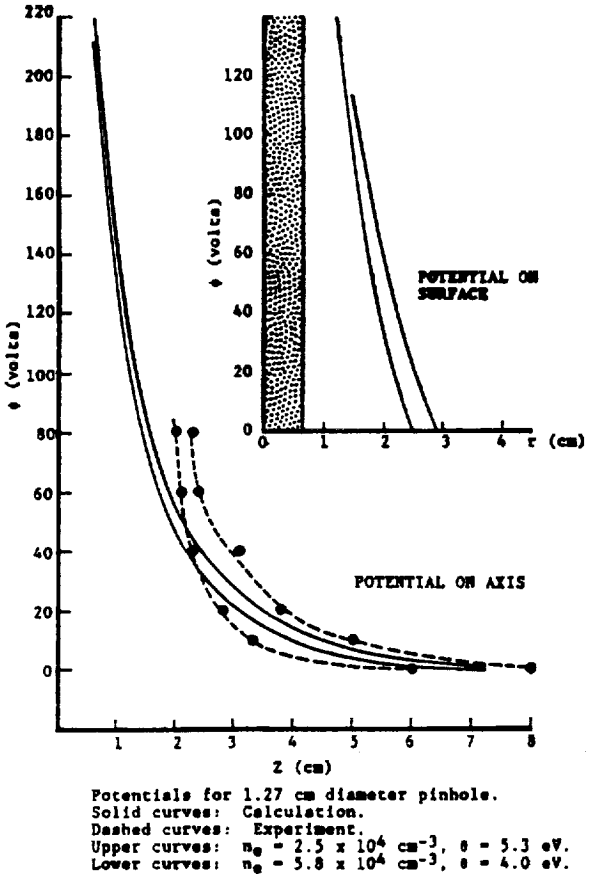

Potentials for 1.27 cm diameter pinhole.
Solid curves: Calculation.
Dashed curves: Experiment.
Upper curves: n_e = 2.5 x 10^4 cm^{-3}, θ = 5.3 eV.
Lower curves: n_e = 5.8 x 10^4 cm^{-3}, θ = 4.0 eV.

Figure 6 Comparison of measured and calculated potentials along the pinhole axis.

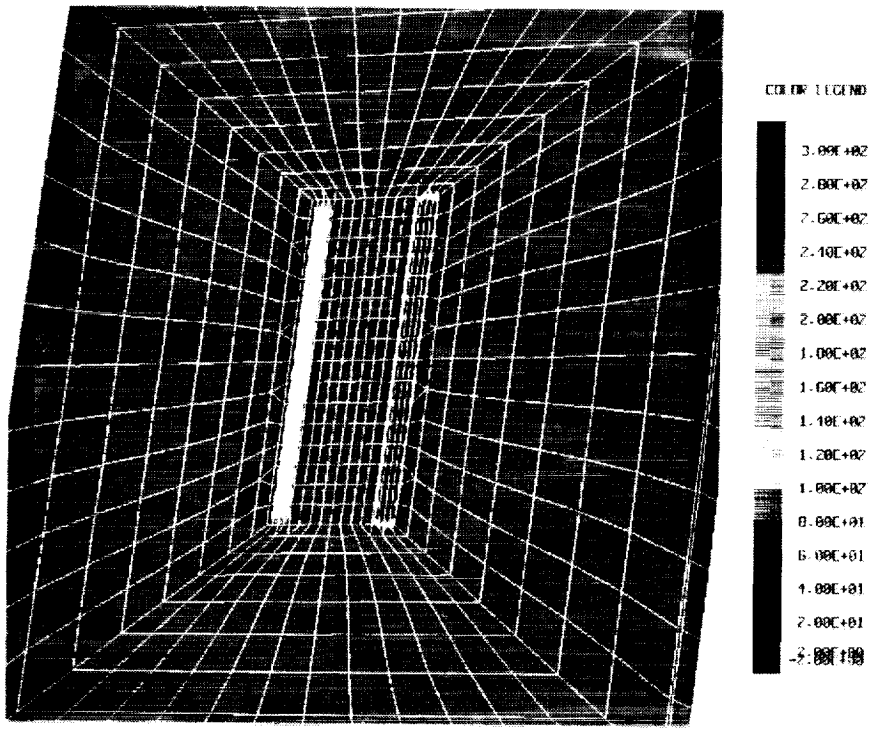

Figure 7 NASCAP/LEO model of the 2-slit experiment, showing surface potentials for the two slits biased at 128 volts and 328 volts.

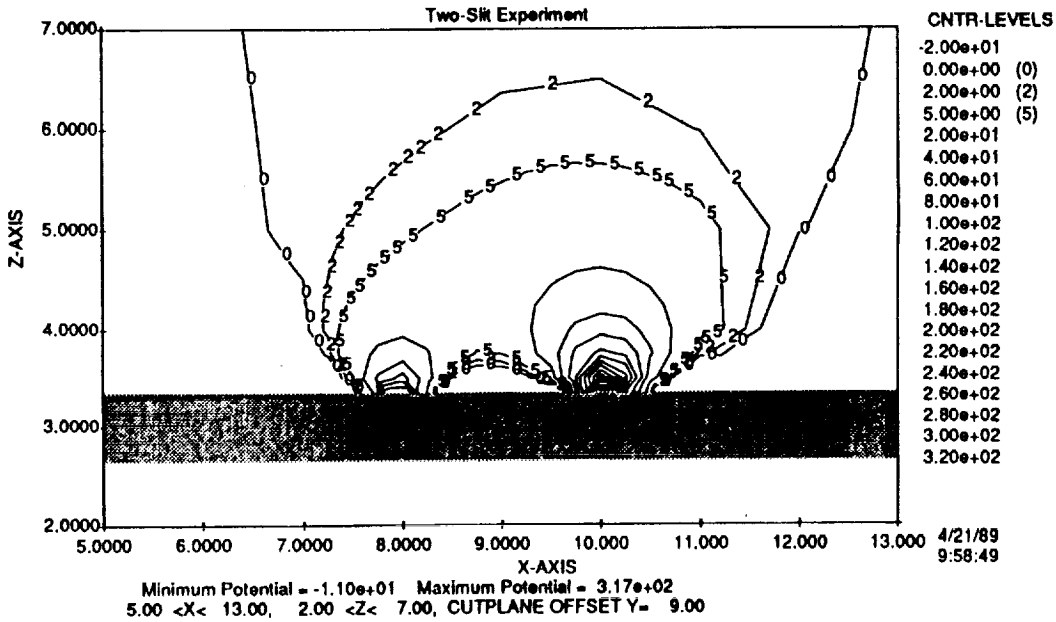

Figure 8 Sheath contour plot showing overlapping sheaths for the bias condition of figure 7. (Note that the bright red region consists of potentials from 20 to 328 volts.)

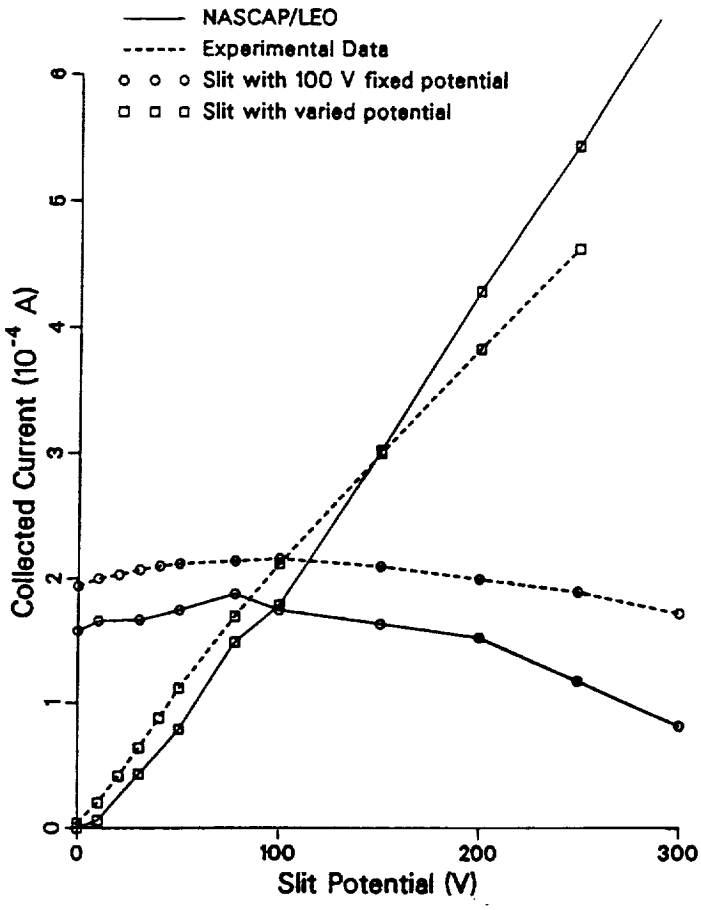

Figure 9 Collected current for two slits with one slit fixed at 100 volts and the second at variable potential.

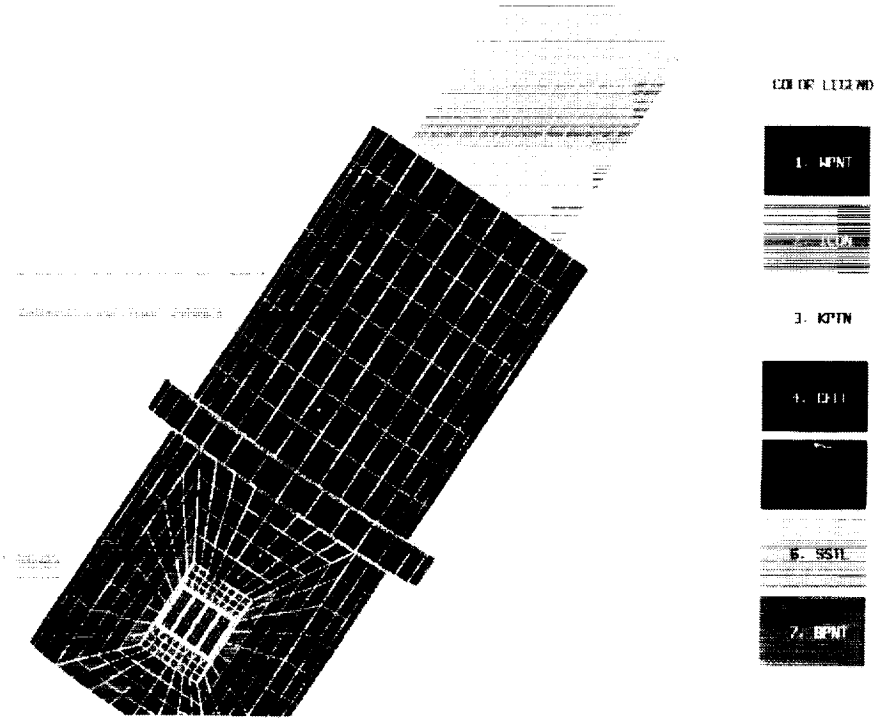

Figure 10 NASCAP/LEO model of PIX-II, showing the solar array sample mounted on rocket body.

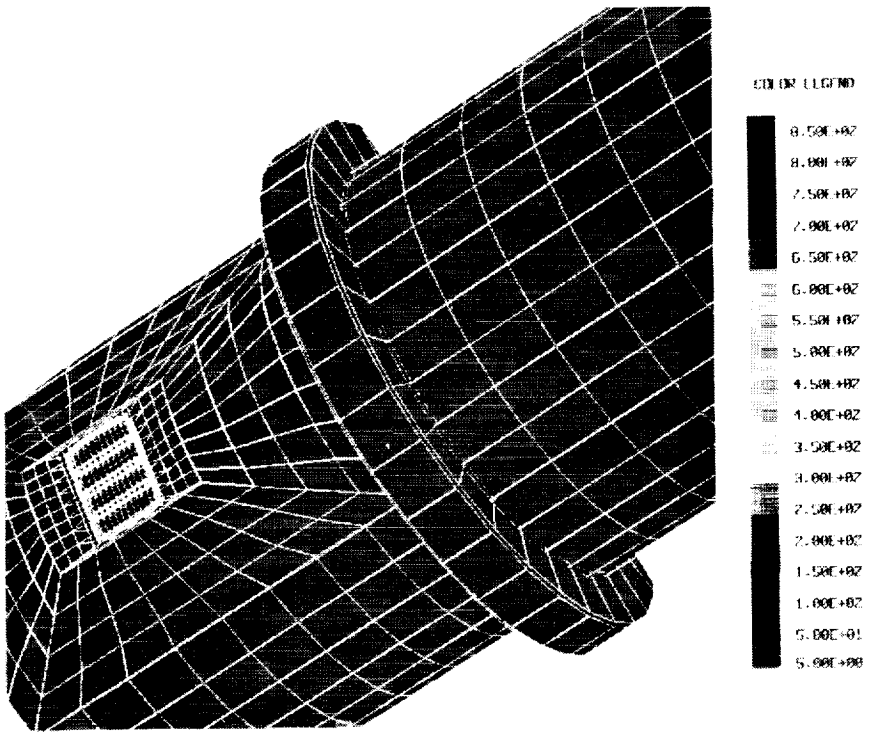

Figure 11 Surface potentials on the solar array sample with interconnects biased to 1,000 volts.

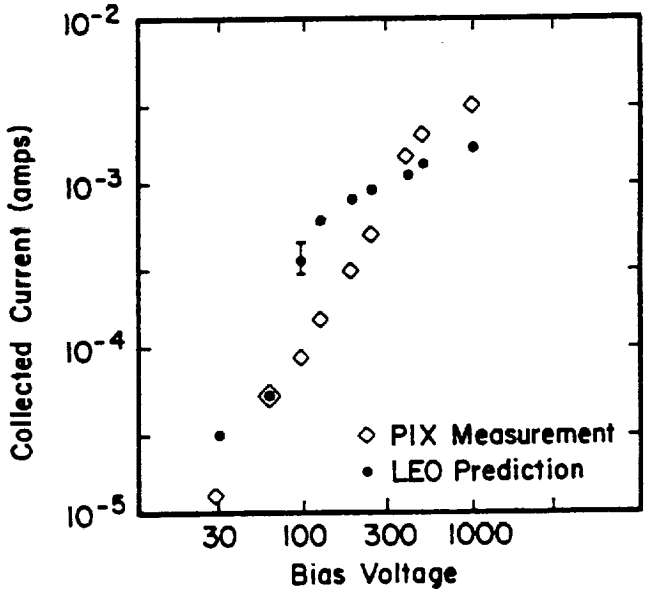

Figure 12 Calculated and measured current collected by the solar array as a function of bias voltage.

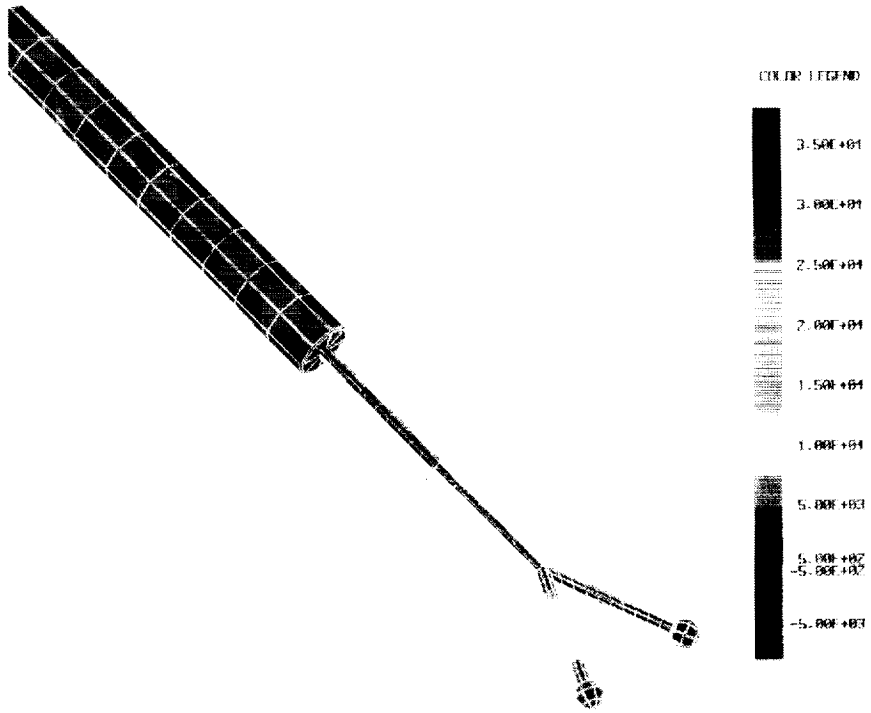

Figure 13 NASCAP/LEO model of SPEAR I, showing the rocket body floating at -8,000 volts and one sphere biased to 46,000 volts.

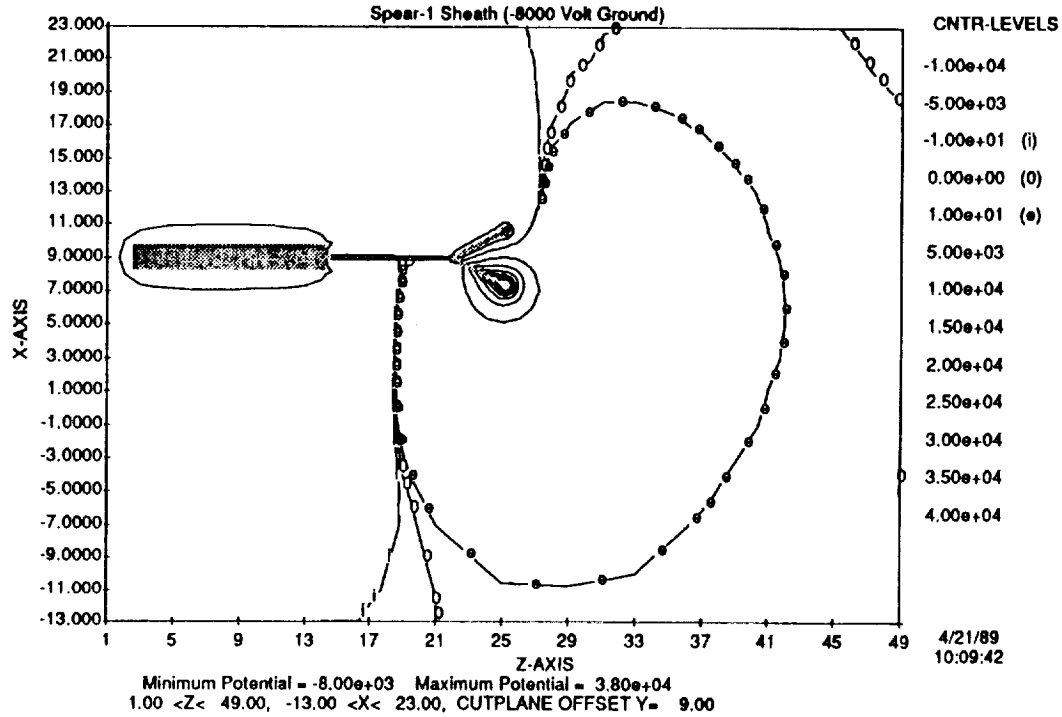

Figure 14 Sheath contour plot showing the asymmetric sheath formed about the probe. (Note that the dark blue region consists of potentials from -8,000 volts to -100 volts, while the bright red region consists of potentials from 100 volts to 38,000 volts.)

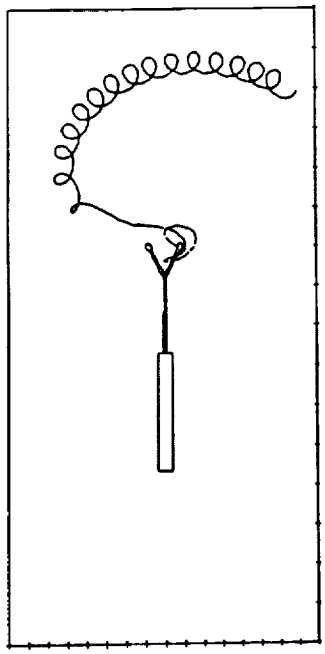

Figure 15 Trajectory of an electron collected by the probe in the asymmetric sheath.

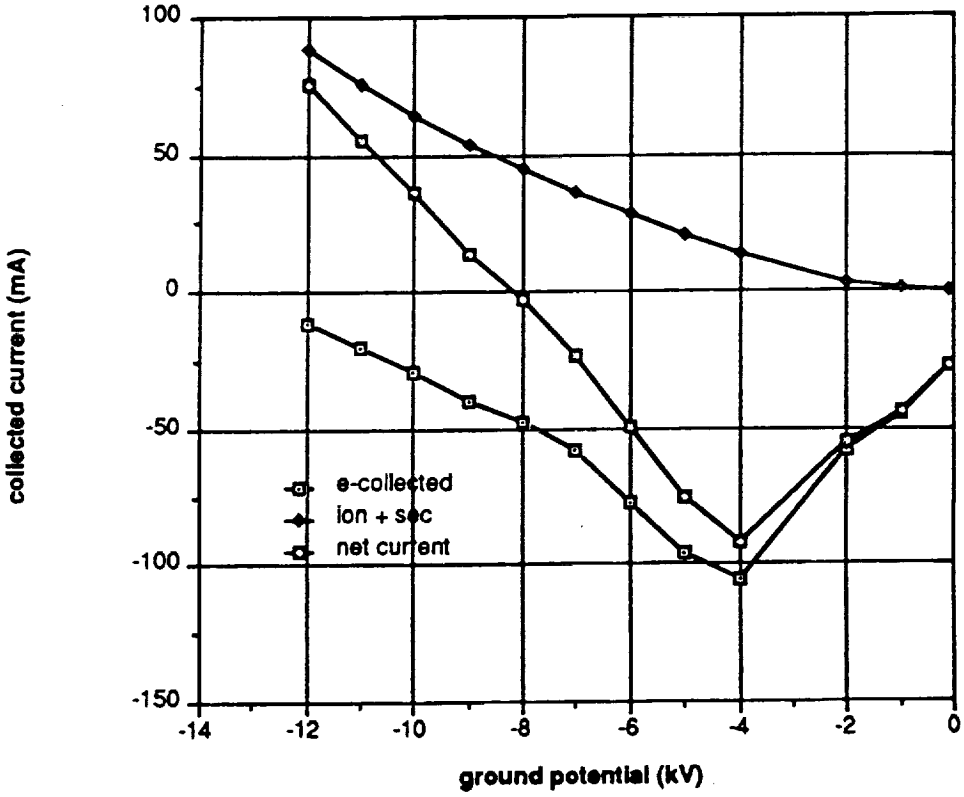

Figure 16 Electron current and secondary-electron-enhanced ion current collected as a function of spacecraft ground potential when 46 kV is applied to one sphere.

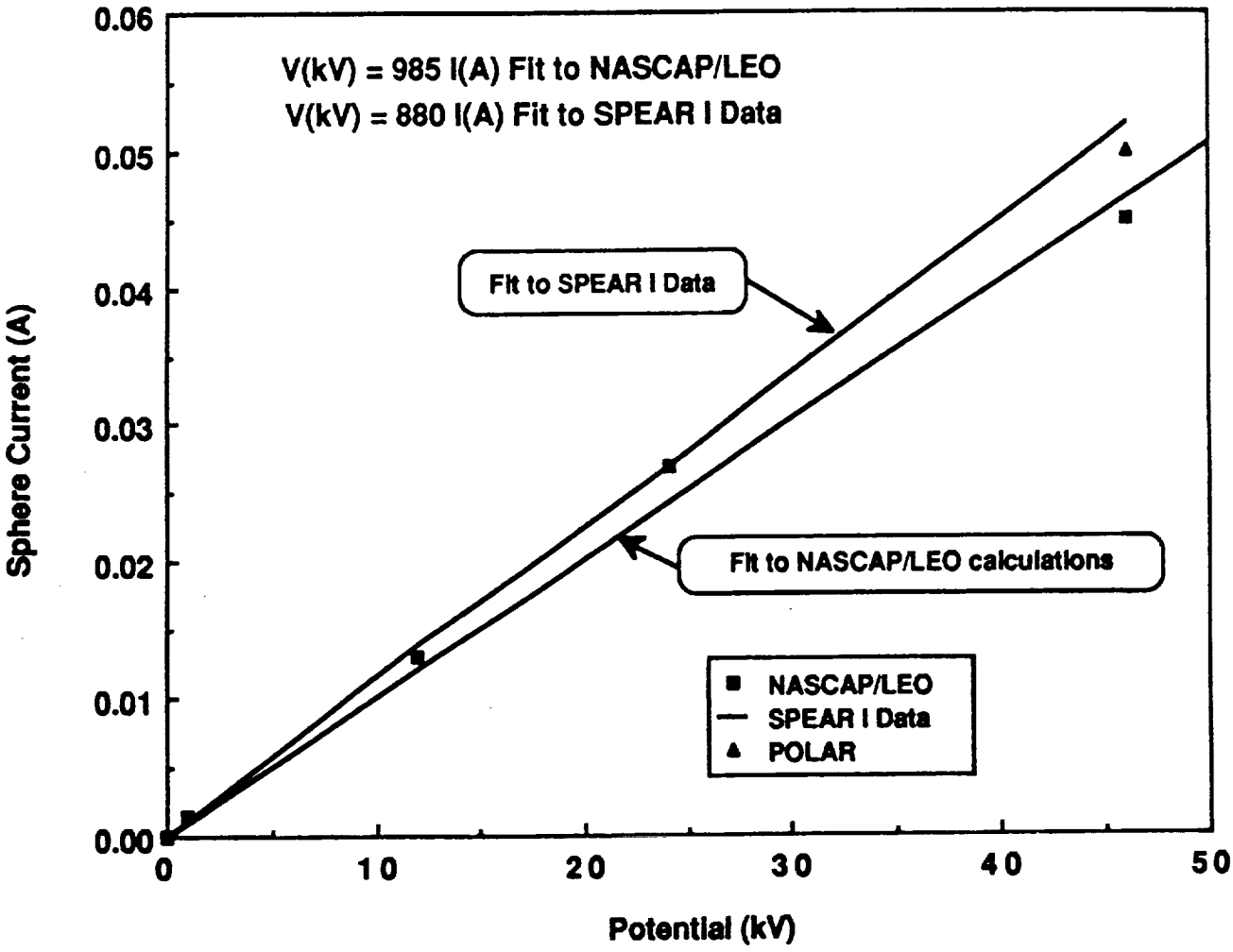

Figure 17 Observed and calculated current collected by the high-voltage sphere.